


Research Article

Folate-Functionalized Thiomeric Nanoparticles for Enhanced Docetaxel Cytotoxicity and Improved Oral Bioavailability

Muhammad Sajjad,¹ Muhammad Imran Khan,¹ Sara Naveed,¹ Sana Ijaz,¹ Omer Salman Qureshi,² Syed Atif Raza,³ Gul Shahnaz,⁴ and Muhammad Farhan Sohail^{1,4,5,6} 

Received 22 October 2018; accepted 28 December 2018; published online 15 January 2019

Abstract. To achieve remotely directed delivery of anticancer drugs, surface-decorated nanoparticles with ligands are reported. In this study, folic acid- and thiol-decorated chitosan nanoparticles loaded with docetaxel (DTX-NPs) were prepared for enhanced cellular internalization in cancer cells and improved oral absorption. The DTX-NPs were explored through *in vitro* and *in vivo* parameters for various parameters. The DTX-NPs were found to be monodisperse nanoparticles with an average particle size of 158.50 ± 0.36 nm, a polydispersity index of 0.36 ± 0.0 , a zeta potential of $+18.30 \pm 2.52$ mV, and an encapsulation efficiency of $71.47 \pm 5.62\%$. The drug release from DTX-NPs followed the *Korsmeyer-Peppas* model with about 78% of drug release in 12 h. In *in vitro* cytotoxicity studies against folate receptor, positive MDA-MBB-231 cancerous cells showed improved cytotoxicity with IC_{50} of $0.58 \mu\text{g/mL}$, which is significantly lower as compared to docetaxel (DTX). *Ex vivo* permeation enhancement showed an efflux ratio of 0.99 indicating successful transport across the intestine. Oral bioavailability was significantly improved as C_{max} and AUC were higher than DTX suspension. Overall, the results suggest that DTX-NPs can be explored as a promising carrier for oral drug delivery.

KEY WORDS: docetaxel; nanoparticles; thiolated chitosan; folic acid; oral bioavailability.

INTRODUCTION

Docetaxel (DTX), an anticancer drug, belongs to the second-generation semisynthetic taxoids clinically used to treat advanced or metastatic breast cancer, gastric cancer, and lung cancer (1,2). DTX interferes with the microtubular network in cells by inhibiting of cell replication and depolymerization, leading to cell seizure during growth cycle at late G₂-M phase and, finally, cell death (3,4). The indications for DTX have been extended recently, to such an extent that in any comprehensive breast cancer chemo cycle, docetaxel is likely to be administered each day of the week and also regularly used in prostate and lung cancers. The oral formulations of DTX are still limited due to its low oral

bioavailability (<5%) which is the result of its extreme lipophilicity and practically insoluble property (4.93 $\mu\text{g/mL}$ in water), hepatic first-pass metabolism, and its high affinity to P-glycoprotein efflux pump (5–7).

The commercial formulation of DTX (Taxotere[®]) is manufactured by adding co-solvent and surfactants that induce some side effects including hypersensitivity, nephrotoxicity, and neurotoxicity (8,9). To overcome these formulation-related problems with drug solubility and permeability, nanotechnology has proven its potential through the development of liposomes, cyclodextrin conjugates, microspheres, polymeric micelles, polymer-drug conjugates, and various kinds of nanoparticles with defined attributes (10,11).

Chitosan, a biodegradable, biocompatible, and cationic natural polysaccharide with low immunogenicity, has been considered as one of the most attractive materials for designing carrier for drugs, antibody, or small interfering RNA (siRNA) owing to its complex forming ability with negatively charged DNA; superior gene transfection, and more efficient protection against stress conditions (12–14). Folate receptors (FRs) are overexpressed in several malignant tumors cells like breast cancer and colon cancer, compared to the normal cells (15). At present, folic acid (FA) has emerged as a potential ligand for receptor-mediated tumor targeting and retains a high affinity for its receptor (16). Folic acid or its conjugates can be taken up by cells *via* endocytosis through the folate receptor, and at the

¹ Riphah Institute of Pharmaceutical Sciences, Riphah International University, Lahore Campus, Lahore, Pakistan.

² Faculty of Pharmacy, University of Lahore, Lahore, Pakistan.

³ College of Pharmacy, University of the Punjab, Lahore, Pakistan.

⁴ Department of Pharmacy, Faculty of Biological Sciences, Quaid-i-Azam University, Islamabad, 45320, Pakistan.

⁵ Department of Chemistry, SBA School of Science and Engineering (SBASSE), Lahore University of Management Sciences (LUMS), Lahore, 54792, Pakistan.

⁶ To whom correspondence should be addressed. (e-mail: pharmacist.pk@gmail.com)

pH 5.0~5.5, the conjugation between folate receptor and folate conjugates breaks down. After that, folate receptors return back to the cell surface and folate conjugates are degraded by lysosome inside the cells (17). The affinity of folate for its cell surface receptor (K_d about 10⁻⁹ M) remains unchanged when it is covalently bonded to a molecule *via* its carboxyl moiety. Therefore, folate-decorated nanoparticles have shown a remarkable enhancement of cellular uptake (18,19).

The present study reports modified chitosan with folic acid and thiol moieties attached to it. The modified polymer was used to synthesize nanoparticles loaded with DTX and aimed to target breast cancer cells through improved cellular internalization, mucoadhesion, and P-glycoprotein (P-gp) efflux pump inhibition. Moreover, the particles were characterized to see the potential for improving oral bioavailability and pharmacokinetics of encapsulated hydrophobic DTX.

MATERIALS AND METHODS

Materials

Low molecular weight chitosan (CS), folic acid, 1-ethyl-3-(3-dimethylaminopropyl)carbodiimide (EDAC), thioglycolic acid (TGA), trimeric sodium phosphate (TPP), Dulbecco's modified Eagle's medium (DMEM), fetal bovine serum (FBS), and 3-(4,5-dimethylthiazolyl-2)-2,5-diphenyltetrazolium bromide (MTT) were purchased from Sigma-Aldrich (Germany). All the other chemicals and solvents used in this study were of research grade and obtained from a variety of vendors. Dialysis membrane having cutoff values 12,000 MWCO were also purchased from Sigma-Aldrich (Germany). The drug DTX was received as a gift from NovaMed Pharmaceuticals (Pvt.), Ltd., Lahore.

Methods

Thiolated Chitosan Synthesis

Chitosan (0.25 g) was dissolved in 500 mL of acetic acid solution (1%, *v/v*) under continuous stirring, and then TGA (1%) and EDAC (50 mM) were added to this mixture. To avoid oxidation during synthesis, hydroxylamine (50 mM) was added. HCl solution (1 M) was used to regulate the pH of the CS solution to 5.0. The reaction mixture was stirred for 4 h to produce thiolated chitosan (TCS). To remove the insoluble impurities, TCS mixture was purified through dialysis under dark conditions using a dialysis tube (cutoff value 12 kDa) at 10 °C for 3 days. This mixture was washed one time with a solution of 5 mM HCl and again washed two times with 5 mM HCl containing 1% NaCl to quench ionic interactions. To adjust the pH at 4.0, the mixture was dialyzed against 1 mM HCl followed by lyophilization and stored at 4 °C until further use (9).

Trinitrobenzenesulfonic Acid Assay for Amine Quantification

Free amino groups present on chitosan, after thiolation, were quantified through trinitrobenzenesulfonic acid (TNBS) assay. Briefly, 1% (*w/v*) solution of TCS was prepared and added with 25 μ L of freshly prepared TNBS reagent. The mixture was kept for 1 h to complete the reaction followed by

evaluation at 420 nm (20). Free amino groups were also quantified after folic acid attachment to the TCS.

Folate-Decorated Thiolated Chitosan Synthesis

EDAC and 10 mg folic acid were dissolved in 5 mL DMSO and dropped into 10 mL deionized water with 1% (*m/v*) TCS. To this, 0.5 M NaOH solution was added to adjust the pH at 9.0 and stirring of the mixture was kept for about 16 h. A mixture of folic acid-decorated thiolated chitosan (FA-TCS) was purified through dialysis using PBS (pH 7.4). Purified FA-TCS was freeze-dried and stored at 4 °C to further use (19). *Quantification of Stabilized Thiol Groups on Thiolated Chitosan.* Quantification of thiol group attached to CS was spectrophotometrically determined using Ellman's reagent (21). Briefly, 0.5 mg of each of CS, TCS, and FA-TCS was dissolved separately in 250 μ L of deionized water. Ellman's reagent and 250 μ L of 0.5 M phosphate buffer solution of pH 8.0 were added to this solution. Thereafter, these samples were subjected to incubation for the period of 3 h at room temperature. Afterward, samples were centrifuged, and the resultant supernatant was moved into a 96-well plate. A spectrophotometer (PerkinElmer, USA) was used to measure the absorbance at the wavelength of 430 nm. TGA was used as the reference standard to calculate the number of immobilized thiol groups.

Estimation of Disulfide Bond. For quantification of total free thiol groups present on TCS and FA-TCS, disulfide content was determined using the previously reported method (22). The disulfide bond was determined by using 0.5 mg of polymer, dissolved in 350 μ L of deionized water. After this, 650 μ L of 0.05 M phosphate buffer solution (pH of 6.8) was added to this mixture. One percent (*m/v*) freshly prepared sodium borohydride (1 mL) solution was added to this mixture. After this, the mixture was incubated at 37 °C for an hour. To decompose the remaining sodium borohydride, 200 μ L of 5.0 M HCl solution was added. One milliliter of 1.0 M phosphate buffer solution having pH 8.5 and 100 μ L of 0.4% (*m/v*) Ellman's reagent in a phosphate buffer having pH 8.0 were also added for neutralization. From this, a 300- μ L aliquot was transferred to a 96-well microplate and absorbance was measured at 430 nm using a microtiter plate reader (PerkinElmer, USA). The amount of free thiol group was determined by subtracting the calculated thiol groups in the earlier step from the total thiol groups immobilized on the modified polymers.

Synthesis of Nanoparticles

Ionic gelation technique was applied for synthesis of nanoparticles following the previously reported method (23). Under continuous stirring, 1 mL of 1% TPP solution was added dropwise to 5% TCS solution containing 1 mg DTX and 1% Tween 80 (used as a wetting agent to increase solubility). The mixture was kept under stirring for 4 h to complete the synthesis of stabilized NPs. After that, the mixture was subjected to dialysis to remove untrapped DTX. DTX-loaded NPs were separated *via* centrifugation and stored at 4 °C.

Blank NPs without drug (to serve as a control) were also synthesized through the same procedure except for adding DTX. **Surface Morphology, Particle Size, Polydispersity Index, and Zeta Potential Analysis.** Particle size, polydispersity index (PDI), and zeta potential of the FA-TCS-NPs and DTX-loaded chitosan nanoparticles (DTX-NPs) were determined by dynamic light scattering using Malvern ZetaNanosizer 3000HS (UK). The surface morphology of DTX-NPs was studied using the scanning electron microscope FEI Nova NanoSEM 450 (USA).

FTIR Analysis of DTX-NPs. Fourier transform infrared spectroscopy (FTIR) was used to check the structural variations in chitosan after attachment of thiol and folic acid moieties. Also, the analysis helped to check the stability of the DTX inside the NPs. A FTIR spectrophotometer (Bruker Alpha-P, USA) was used for this purpose.

Encapsulation Efficiency. For encapsulation efficiency (EE), 2 mg of lyophilized DTX-NPs was resuspended in Tris HCl buffer solution and suspension was subjected to sonication for 30 min. After this, 1 mL of HPLC mobile phase (acetonitrile:methanol:buffer) was added into this mixture and again sonicated for the next 15 min to extract drug into the mobile phase. The resultant solution was filtered through a 0.22- μ m syringe filter and was transferred to a HPLC vial. Chromatographic separation was achieved by using Waters HPLC (Waters e2695, USA) with a 10- μ l injector (automatic), and UV-visible with a PDA detector (Waters 2998, USA) was attached along with a fraction collector. Waters Spherisorb C₁₈ (5 μ m, ODS2 4.6 \times 250 mm) column was used for the separation. The output signal was monitored and integrated using Empower 5.0 software. The mobile phase consisting of acetonitrile, methanol, and acetate buffer (10 mM, pH 5.0) in a ratio of 48:16:36 (v/v/v), respectively, was filtered through a 0.45- μ m membrane filter and degassed by sonication for 30 min. The solvent was pumped from the reservoir under isocratic condition (100%) into the C₁₈ column at a flow rate of 0.8 mL/min. The column and sample

temperature were set at 25 \pm 0.5 $^{\circ}$ C. Detection was done at 230 nm, and the sample run time was 10 min (9).

$$\text{Encapsulation efficiency} = \frac{\text{Amount of drug in formulation}}{\text{Total amount of drug}} \times 100$$

In Vitro Drug Release Studies. The dialysis membrane method was employed to determine the *in vitro* drug release from DTX-NPs. The weighed quantity of DTX and DTX-NPs containing drug equivalent to 5 mg was taken and resuspended in deionized water. The dialysis membrane of a cutoff value of 12 kDa was used. The DTX-NPs were placed in dialysis membrane, sealed, and then immersed in 30 mL of 0.1 M phosphate buffer solution having pH 7.4. As DTX has less solubility in phosphate buffer solution, 1% (m/v) Tween 80 was also added to maintain the sink conditions. The whole system was maintained at the temperature of 37 $^{\circ}$ C \pm 0.5 and 100 rpm. The samples were withdrawn at regular intervals. These samples were filtered by using a 0.22- μ m syringe filter and then analyzed through HPLC using the method reported for determination of encapsulation efficiency.

Cytotoxicity Assay. *In vitro* cytotoxicity of DTX-NPs was conducted on MDA-MB-231 breast cancer cell line through MTT assay (24,25). Briefly, MDA-MB-231 cells were seeded in a 96-well multiplate having a density of 6000 cells in a well-prepared solution of DMEM and FBS and then incubated with varying concentrations (0.1 μ g/mL to 100 μ g/mL) of DTX and DTX-NPs containing an equivalent amount of DTX and FA-TCS-NPs as an internal control for 24 h. After this, the medium was removed and 10 mL of a fresh solution of DMEM and MTT was added in each well and again incubated for the next 4 h. After that, the medium was removed and, finally, 100 μ L of DMSO was added in each well to dissolve the formazan crystals produced by living cells and then absorbance was measured by using a multiplate reader (PerkinElmer, USA) at 570 nm. Inhibition concentration for 50% cell death (IC₅₀) was then calculated using GraphPad Prism software (version 6.0).

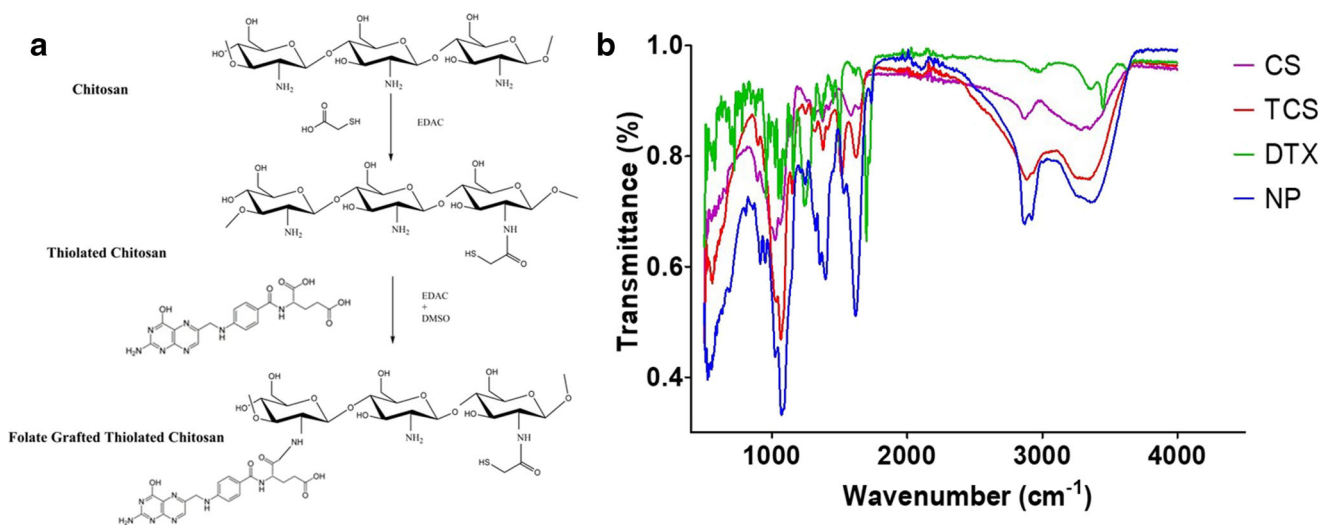


Fig. 1. a FTIR spectra of chitosan (CS), thiolated chitosan (CS-TGA), pure drug (DTX), and drug-loaded nanoparticles (DTX-NPs). b Particle size distribution chart. c Zeta potential distribution chart

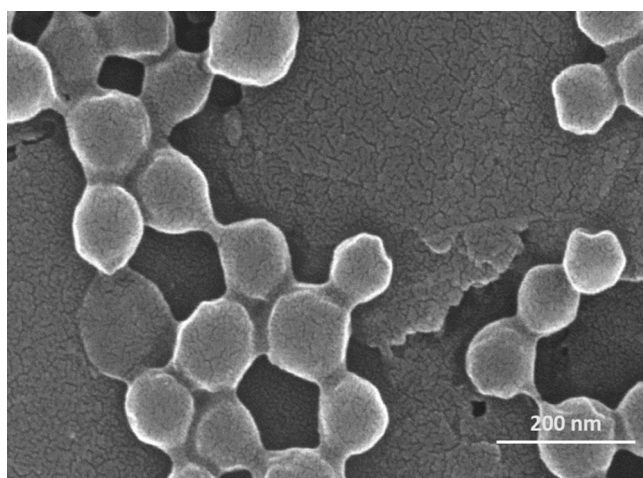


Fig. 2. Scanning electron microscopy (SEM) images of DTX-NPs showing smooth surface and round morphology

Ex Vivo Permeation Enhancement and Efflux Pump Inhibition Analysis. *Ex vivo* permeation studies of DTX-NPs were performed using an everted sac (26). Briefly, freshly excised intestine of the rat was obtained, thoroughly washed with Krebs-Ringer solution (pH 6.5), and cut into pieces of 4–5 cm. The intestine was everted by carefully passing through it a narrow glass rod and stored in oxygenated Krebs-Ringer solution at 4 °C till further use. Each segment was tied at one end with silk suture, and 1 mL of the sample (1 mg/mL) was carefully filled in the sac using a hypodermic syringe, while the other end was tied with silk suture. Verapamil (100 µg/mL), a P-gp inhibitor, was filled in one sac to compare the apparent permeation enhancement of DTX-NPs. All filled sacs were immersed in tubes filled with 10 mL of oxygenated Krebs-Ringer solution and incubated at 37 °C under gentle mechanical shaking. The samples were collected from the surrounding medium at a definite time and replaced with the same amount of fresh solution. The collected samples were analyzed using the HPLC method described earlier.

$$\text{Apparent permeability (g/cm}^2\text{)} = \frac{\text{Concentration} \times \text{Volume}}{\text{Mucosal area}}$$

The mucosal surface area was calculated by assuming intestine a cylinder and using the following formula:

$$\text{Mucosal surface area (cm}^2\text{)} = \text{circumference } (\pi r^2) \times \text{length}$$

Oral Pharmacokinetic Evaluation. The oral pharmacokinetic studies were performed as per the approved protocol by the ethical committee of Riphah International University, Lahore, Pakistan. Rabbits were divided into two groups ($n =$

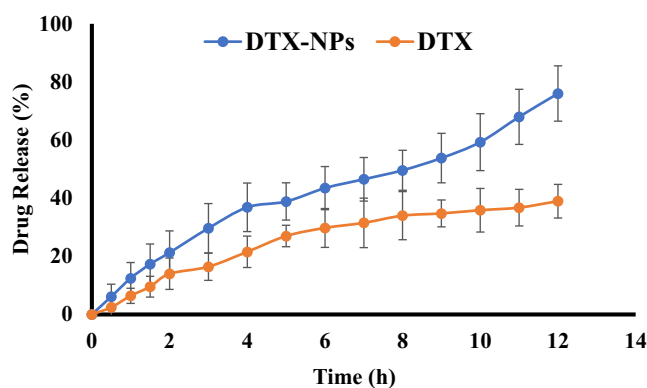


Fig. 3. *In vitro* drug release of pure DTX from DTX suspension. Studies of DTX-NPs performed using the dialysis method in phosphate buffer (pH 7.4) for 72 h. The results are presented as mean \pm SD of three analysis

5). Group 1 was orally administered with DTX suspension, and group 2 was treated with DTX-NPs. The animals were housed with free access to food and water. After predefined intervals, the blood was carefully withdrawn and centrifuged to separate plasma. The drug was extracted from the plasma using the mobile phase through the liquid-liquid extraction method and analyzed using the HPLC method reported for encapsulation efficiency.

RESULTS AND DISCUSSION

Synthesis and Characterization of Thiolated Chitosan

Chemical alteration of chitosan structure with functional groups can be useful to augment its physicochemical properties. Most of these chemical modifications are carried out at its primary amino group because of its electron donating effect with other functional groups such as carboxylic acids (27). Many chemical processes have been developed to get chitosan derivatives. Thiol modification of chitosan is widely used in order to improve bulk polymer properties such as mucoadhesion, solubility, and cellular permeation. The attachment of thiol group at chitosan backbone enables the development of a disulfide bond (both internal and external), resulting to being a multifunctional biomaterial (28). The grafting of folic acid with CS-TGA was based on the mechanism of carbodiimide chemistry (Fig. 1a) in which EDAC was used to activate the carboxylic group of folic acid, resulting in an amine reactive intermediate called *O*-acylisourea. Afterward, TCS was formed from the reaction between *O*-acylisourea and the free amino groups of thiolated chitosan. The number of total thiol groups

Table 1. Results of Particle Size, Polydispersity Index (PDI), Zeta Potential, and Encapsulation Efficiency of NP and DTX-NP Formulation Synthesized

Formulations	Particle size (nm)	PDI	Zeta potential (mV)	Encapsulation efficiency (%)
TCS-NPs	118.50 \pm 3.34	0.21 \pm 0.01	+ 21.10 \pm 0.34	–
DTX-NPs	158.50 \pm 0.36	0.36 \pm 0.01	+ 18.30 \pm 2.52	71.47 \pm 5.62

Results are shown in triplicate as mean \pm SD

Table II. Pharmacokinetic Modeling Based on *In Vitro* Drug Release Data of Various Formulations Synthesized to Determine Drug Release Mechanism from NCs

Formulations	Zero order		Korsmeyer-Peppas		Higuchi		Hixon-Crowell	
	R^2	K_0	R^2	N	R^2	K_H	R^2	K_{HC}
DTX	0.46	1.31	0.98	0.39	0.94	9.15	0.70	0.05
DTX-NPs	0.58	1.65	0.98	0.43	0.96	11.40	0.88	0.01

immobilized on TCS and free thiol groups present was found to be an average of $845 \pm 67 \mu\text{M}$ thiol groups and $128 \pm 73 \mu\text{M}$ per g of TCS, respectively. Primary amine quantification showed $76.43 \mu\text{M/g}$ of primary amine present on TCS. TCS was obtained by lyophilization as white odorless material and then stored at 4°C . This lyophilized polymer was found stable towards oxidation throughout the period of this study.

Synthesis and Characterization of Folic Acid-Grafted Thiolated Chitosan

The synthesis of FA-TCS was based on the carbodiimide chemistry similar to what was used for attaching thiol groups (Fig. 1a). EDAC successfully activated carboxylic groups of folic acid to generate an intermediate an active *O*-acylisourea. This active intermediate was displaced with primary amino groups of chitosan through nucleophilic substitution reaction, and amide bond was formed between the primary amine and carboxylic groups of folic acid. FA-TCS appeared as yellow-colored material. The quantification of free thiol groups after FA attachment was found to be $158 \pm 47 \mu\text{M}$ per g of TCS. TNBS assay showed $32.42 \mu\text{M/g}$ primary amine present in FA-TCS. This gave a confirmation of successful FA attachment to the TCS, resulting in FA-TCS. This was further confirmed through FTIR analysis of all polymer grafts.

FTIR Analysis of Formulations

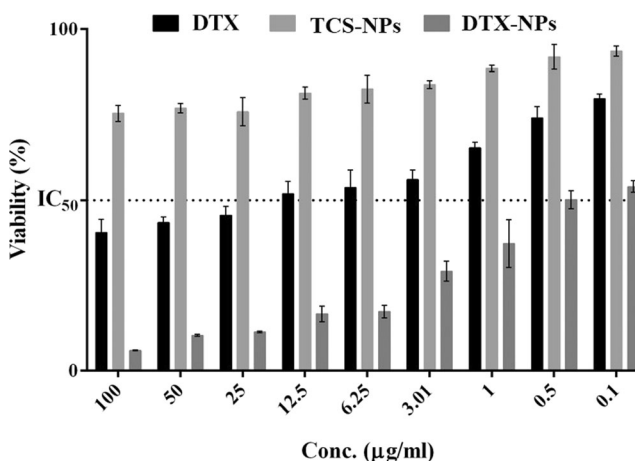
Figure 1b presents the FTIR spectra of CS, TCS, FA-TCS, and DTX-NPs. Results of FTIR analysis showed the fruitful modification of pure chitosan into thiolated chitosan by the reaction between the primary $-\text{NH}_2$ groups of native chitosan and the $-\text{COOH}$ groups of the TGA. A strong band in the region of $3290\text{--}360 \text{ cm}^{-1}$ is due to the presence of N-H and O-H stretching and hydrogen bonding as well. The absorption bands at 1654 cm^{-1} represent amide I, and at 3230 cm^{-1} , deformation of signal due to the $-\text{NH}$ stretching amide indicates the formation of a C-NH amide bond. The peaks at 1604 cm^{-1} show the presence of an amino group (NH_2) whereas the absorbance bands at 1382 cm^{-1} correspond to the presence of amide III. The absorption

Table III. IC_{50} Values of DTX Suspension and DTX-NPs Against MBA-231 Cell Line Calculated from Cytotoxicity Data Using GraphPad Prism Software 6.0

Formulation	IC_{50} value ($\mu\text{g/mL}$)
DTX	13.62 ± 3.31
DTX-NPs	0.58 ± 0.18

* represents $p < 0.001$

band at 2498 cm^{-1} ($-\text{SH}$ stretching) corresponds to the presence of thiol group linked at the terminal of chitosan. The existence of the S-S disulfide bond in TCS was confirmed by the peak at 804 cm^{-1} and C-SH stretching peak at 1240 cm^{-1} since these peaks were absent in CS spectra. The spectrum of TCS showed the absorbance bands at 3351 cm^{-1} and 3209 cm^{-1} because of the stretching of N-H and O-H functional groups. The absorbance bands at 1630 cm^{-1} represented *N*-acetyl groups, and the intensity of peak near 1604 cm^{-1} reduced which indicates the partial conjugation of the amino group to TGA. The FTIR spectrum of FA-TCS showed the characteristic absorbance bands at 3372 cm^{-1} which corresponds to that of an alcohol group (O-H stretching). Another characteristic absorbance peak at 3274 cm^{-1} represents the primary amine group ($-\text{NH}_2$) and the secondary amine group ($-\text{NH}$) present in the structure (N-H stretching). The peak at 1662 cm^{-1} in the spectrum represented the presence of the carbonyl group (C=O stretching) whereas the absorbance bands at 1585 cm^{-1} represent (N-H) bending in the secondary amine. The appearance of a new characteristic peak at 1315 cm^{-1} corresponds to the C-N stretching of secondary amine. Hence, all data of the FTIR spectrum showed that free amino groups (NH_2) of chitosan thioglycolic acid were successfully converted to NH. Moreover, the FTIR spectra of pure DTX showed an absorbance band at 3445 cm^{-1} , indicating the N-H group and characteristic peak at characteristic peaks at 3340 cm^{-1} correspond to O-H stretching. The peak of the carbonyl functional group C=O appeared at

**Fig. 4.** *In vitro* cytotoxicity comparison of DTX suspension with DTX-NPs and FA-TCS-NPs showing the highly improved effect on MDA-MB-231 cell line using MTT assay. The IC_{50} values of DTX and DTX-NPs were $13.62 \mu\text{g/mL}$ and $0.58 \mu\text{g/mL}$, respectively. FA-TCS-NPs showed no effect on cell killing

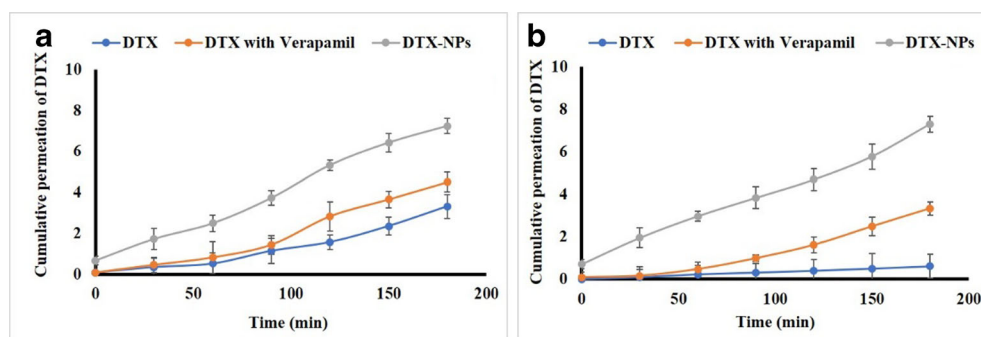


Fig. 5. *Ex vivo* permeation enhancement study. **a** Basolateral to apical surface and **b** apical to basolateral surface, showing improved permeation with DTX-NPs as compared to DTX suspension and DTX in the presence of verapamil

1720 cm^{-1} whereas the absorbance bands due to aromatic and aliphatic carbon atoms (C–H) appeared to be C–H in the range of 2805 cm^{-1} and 3065 cm^{-1} . These characteristic peaks of drug incorporated in nanoparticles established that DTX is still present in our formulation as a chemically unchanged form.

Synthesis and Characterization of DTX-NPs

The DTX-NPs were successfully synthesized using the ionic gelation method. The particle size was measured from the scanning electron microscopy (SEM) images by using ImageJ software. The hydrodynamic size of NPs and DTX-NPs was 118.50 ± 3.34 and 158.50 ± 0.36 , and the polydispersity index value was 0.21 ± 0.01 and 0.36 ± 0.01 , respectively. The zeta potential value represented the repulsive or attractive interactions between adjacent particles, and the modulation of charge plays a vital role to design a nanodevice able to interact with a negative or positive membrane barrier of cells. The value of surface zeta potential was $+21.10 \pm 0.34$ and $+18.30 \pm 2.52$ for NPs and DTX-NPs, respectively. DTX-NPs exhibited a larger particle size owing to the presence of folic acid and thiol groups on the DTX-NPs. The surface zeta potential value of FA-CS-NPs was positive ($+18.30 \pm 2.52$), and particles showed good stability at room temperature. An analysis of the morphology of DTX-NPs was done by SEM as shown in Fig. 2 which shows a semispherical appearance with a smooth surface. The particles appear to be homogenized and monodispersed nanoparticles. The encapsulation efficiency of the DTX-NPs was found to be $71.47 \pm 5.62\%$ as shown in Table I.

In Vitro Drug Release Studies

Controlled drug release ensures the smooth blood concentration of a drug over an extended time period which

reduces dose frequency, minimizes side effects, maximizes therapeutic efficacy, and improves patient compliance. An *in vitro* drug release study was performed to see the release pattern of DTX from DTX-NPs. The study was conducted by the sink condition dialysis membrane method for the period of 12 h at a physiological pH value of 6.8. The cumulative drug release from DTX-NPs in terms of percentage was calculated against predetermined time intervals (Fig. 3). The results showed that the controlled DTX release from DTX-NPs as indicated around 60% release was observed within 12 h. The release kinetic models were applied to determine the drug release pattern from DTX-NPs as shown in Table II which contains R^2 and K values of all release kinetic models. The value of R^2 which suggested a pattern of drug released from DTX-NPs according to the Korsmeyer-Peppas model ($R^2 = 0.956$) and the n value less than 0.45 showed a Fickian release kinetics. Incorporated docetaxel-loaded nanoparticles exhibit smooth sustained continuous release of drug up to 12 h because of the formation of covalent cross-linking of disulfide bonds inside the DTX-NPs during the swelling process.

In Vitro Cytotoxicity

Many human cancer cells like lung, ovarian, chest, and colon have highly overexpressed with folate receptors to achieve the remotely highly targeted drug delivery of many anticancer agents. Folate receptors are present on the cell membrane of malignant cells which allows nanoparticles inside the cell *via* endocytosis. Since the last few decades, folic acid has appeared as an attractive ligand as tumor-targeted therapy because the attraction of folate for its cell surface receptor remains unchanged when it is covalently bonded to a molecule *via* its carboxyl moiety (29). Therefore, folate-grafted modified nanoparticles showed a remarkable improvement of cell endocytosis as compared with surface

Table IV. *Ex Vivo* Permeation Enhancement Studies of Basolateral to Apical (B-A) and Apical to Basolateral (A-B) Surface of Rat Intestine and Apparent Permeability and Improvement Ratio of DTX-NPs as Compared to DTX Suspension and DTX in the Presence of Verapamil

Formulations	p_{app} (A-B) (cm/s) $\times 10^{-6}$	Improvement ratio	p_{app} (B-A) (cm/s) $\times 10^{-6}$	Improvement ratio	Efflux ratio = B-A/A-B
DTX suspension	0.089 ± 0.03	–	0.479 ± 0.37	–	5.38
DTX-verapamil	0.482 ± 0.41	5.36	0.651 ± 0.62	1.36	1.35
DTX-NPs	$1.057^* \pm 0.51$	11.75	$1.047^* \pm 0.87$	2.18	0.99

The results are shown as mean \pm SD of three results

* represents $p < 0.001$

unmodified nanoparticles. In this study, pure DTX and DTX-NPs were investigated on *MDA-MB-231* cells by MTT assay. The results showed that the DTX-NPs have more cellular uptake ability as compared to another pure drug due to the fact of phagocytosis *via* folate receptor through the ligand receptor-mediated interaction and thus increased the intracellular concentration of the DTX. The results showed significantly improved cytotoxicity with DTX-NPs as compared to DTX suspension. IC_{50} value for DTX and DTX-NPs was 13.6 $\mu\text{g/mL}$ and 0.065 $\mu\text{g/mL}$, respectively (Table III, Fig. 4). This superiority might be attributed to the inhibition of efflux pump by thiol groups ($-\text{SH}$) along with better cellular uptake *via* folic acid receptor-mediated internalization and retaining drug inside the cell. It has been shown by many other studies that the surface-modified nanoparticles have higher cytotoxicity as compared to surface-unmodified nanoparticles. The results of this study showed that surface-modified DTX-NPs have strong targeting ability, more cellular uptake, and enhanced cytotoxic effects as compared to the pure drug, DTX.

Ex Vivo Permeation Enhancement and Efflux Pump Inhibition Analysis

Intestinal absorption is a rate-limiting step which needs to be addressed to improve the oral bioavailability of drugs. A large number of intestinal influx and efflux transporters are present to control oral bioavailability (30). P-gp that is present on the basolateral side of the intestine plays an important role as an efflux pump for DTX (31). Therefore, the permeation enhancement effect of DTX-NPs by inhibiting P-gp was evaluated in comparison of verapamil (P-gp inhibitor). The results shown in Fig. 5 demonstrated that in the presence of verapamil (100 $\mu\text{g/mL}$), DTX absorption was markedly increased by 4.2-fold ($p < 0.05$). The Papp enhancement ratio from apical to basal was 11.06-fold higher for the DTX-NPs. The efflux ratio was found to be 0.99 as shown in Table IV. This suggested the involvement of a possible mechanism of permeation improvement by thiolated polymers *via* protein tyrosine phosphatase (PTP) inhibition through the disulfide bond (S-S) development between the cysteine of the protein (23). Subsequently, increased tyrosine

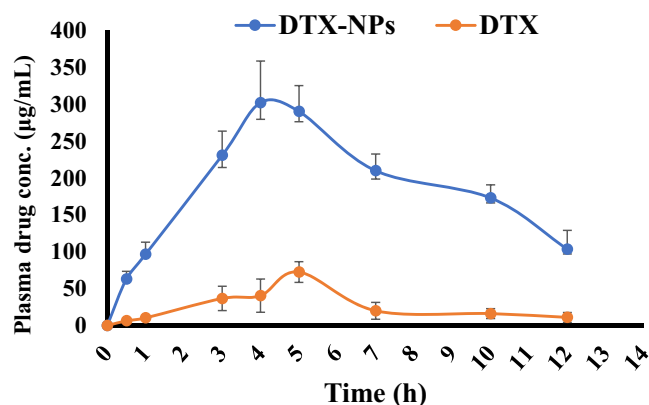


Fig. 6. Plasma concentration of DTX after oral administration of DTX suspension and DTX-NPs (oral dose = 10 mg/kg). Blood samples were taken at a predefined time till 12 h and analyzed through HPLC for DTX quantification

Table V. *In Vivo* Bioavailability and Different Pharmacokinetic Parameters Obtained After Oral Administration of Formulations to Rabbit and Analyzing Plasma Samples Through HPLC

PK parameter	Unit	DTX	DTX-NPs
C_{\max}	$\mu\text{g/mL}$	72.56	302.06
T_{\max}	h	4	4
$t_{1/2}$	h	6.07	5.47
AUC_{0-t}	$\mu\text{g/mL/h}$	322.84	2295.92
MRT	h	9.04	9.65

phosphorylation of the occluding membrane protein contributes to the opening of the intestinal tight junctions resulting in improved permeability through the paracellular route. Hence, the P-gp inhibition *via* TCS-based nanoparticles could be a promising strategy to enhance DTX permeation.

Oral Pharmacokinetic Evaluation

The DTX-NPs were aimed to improve the pharmacokinetic profile of DTX through improved oral permeation across enterocytes that was assessed in healthy rabbits. Oral absorption of NPs and xenobiotics through the GIT is facilitated by villus tips that can allow particles of the size range 5–150 μm to cross easily, while intestinal macrophages may facilitate transport of NPs up to 1 μm and enterocytes may allow particles of about 300 nm through transcellular route (32). Drug solubility in GIT fluid is the rate-limiting step for orally administered formulations to reach systemic circulation across the intestinal barrier. These DTX-NPs were, therefore, able to increase the permeability and solubility of hydrophobic DTX. Plasma drug concentrations achieved at various time intervals, following oral administration of DTX-NPs, are shown in Fig. 6. The different calculated pharmacokinetic parameters are present in Table V. Following oral administration, the C_{\max} of DTX suspension reached 72.56 $\mu\text{g/mL}$ after 5 h whereas the DTX-NPs achieved the C_{\max} of 302.06 $\mu\text{g/mL}$ in 4 h and remained within the therapeutic for a longer duration. DTX plasma levels from DTX-NPs were below the minimum toxic concentration (2700 ng/mL) as observed after intravenous administration of DTX and reported earlier (33). The half-life ($t_{1/2}$) of DTX-NPs was 5.47 h. The AUC_{0-96} of DTX-NPs showed the increased oral bioavailability, *i.e.*, 7.5-fold as compared to DTX suspension. This improved oral pharmacokinetics of DTX from DTX-NPs might owe to various underlying mechanisms of FA-TCS involving augmented mucoadhesion, inhibition of P-gp, and enhanced paracellular transport through enterocytes. Furthermore, the particle size, *i.e.*, ~158 nm, might have also facilitated the paracellular transport through the gastric mucosa (9).

CONCLUSION

The new polymeric graft (FA-TCS) having thiol and folic acid groups was successfully developed and characterized for its physiochemical properties. The nanoparticles developed using FA-TCS successfully encapsulated hydrophobic drug and appeared as uniformly synthesized smooth nanoparticles with improved cytotoxicity towards folic acid-overexpressed breast cancer cells. Moreover, the particles were able to

enhance the oral permeation, thus increasing the bioavailability and pharmacokinetic profile of DTX. Overall, these newly developed polymeric nanoparticles have proven their potential for drug delivery of hydrophobic cytotoxic drugs with site specificity that could be further investigated and a new carrier system was developed for oral delivery of anticancer drugs.

COMPLIANCE WITH ETHICAL STANDARDS

Conflict of Interest The authors declare that they have no conflict of interest.

Publisher's Note Springer Nature remains neutral with regard to jurisdictional claims in published maps and institutional affiliations.

REFERENCES

- Montero A, Fossella F, Hortobagyi G, Valero V. Docetaxel for treatment of solid tumours: a systematic review of clinical data. *Lancet Oncol*. 2005;6(4):229–39.
- Kintzel PE, Michaud LB, Lange MK. Docetaxel-associated epiphora. *Pharmacotherapy*. 2006;26(6):853–67.
- Gueritte-Voegelein F, Guenard D, Lavelle F, Le Goff MT, Mangatal L, Potier P. Relationships between the structure of taxol analogs and their antimetabolic activity. *J Med Chem*. 1991;34(3):992–8.
- Ringel I, Horwitz SB. Studies with RP 56976 (taxotere): a semisynthetic analogue of taxol. *J Natl Cancer Inst*. 1991;83(4):288–91.
- Kuppens I, Bosch T, Van Maanen M, Rosing H, Fitzpatrick A, Beijnen J, et al. Oral bioavailability of docetaxel in combination with OC144-093 (ONT-093). *Cancer Chemother Pharmacol*. 2005;55(1):72–8.
- Gao K, Sun J, Liu K, Liu X, He Z. Preparation and characterization of a submicron lipid emulsion of docetaxel: submicron lipid emulsion of docetaxel. *Drug Dev Ind Pharm*. 2008;34(11):1227–37.
- Sohail MF, Rehman M, Sarwar HS, Naveed S, Salman O, Bukhari NI, et al. Advancements in the oral delivery of docetaxel: challenges, current state-of-the-art and future trends. *Int J Nanomedicine*. 2018;13:3145–61.
- Lee E, Kim H, Lee I-H, Jon S. In vivo antitumor effects of chitosan-conjugated docetaxel after oral administration. *J Control Release*. 2009;140(2):79–85.
- Sohail MF, Javed I, Hussain SZ, Sarwar S, Akhtar S, Nadhman A, et al. Folate grafted thiolated chitosan enveloped nanoliposomes with enhanced oral bioavailability and anticancer activity of docetaxel. *J Mater Chem B*. 2016;4(37):6240–8.
- Jain A, Thakur K, Kush P, Jain UK. Docetaxel loaded chitosan nanoparticles: formulation, characterization and cytotoxicity studies. *Int J Biol Macromol*. 2014;69:546–53.
- Hassan S, Prakash G, Ozturk AB, Saghadzadeh S, Sohail MF, Seo J, et al. Evolution and clinical translation of drug delivery nanomaterials. *Nano Today*. 2017;15:91–106.
- Gao Y, Liu X-L, Li X-R. Research progress on siRNA delivery with nonviral carriers. *Int J Nanomedicine*. 2011;6:1017.
- Mansouri S, Lavigne P, Corsi K, Benderdour M, Beaumont E, Fernandes JC. Chitosan-DNA nanoparticles as non-viral vectors in gene therapy: strategies to improve transfection efficacy. *Eur J Pharm Biopharm*. 2004;57(1):1–8.
- Hamed H, Moradi S, Hudson SM, Tonelli AE. Chitosan based hydrogels and their applications for drug delivery in wound dressings: a review. *Carbohydr Polym*. 2018;199:445–60.
- Weitman SD, Lark RH, Coney LR, Fort DW, Frasca V, Zurawski VR, et al. Distribution of the folate receptor GP38 in normal and malignant cell lines and tissues. *Cancer Res*. 1992;52(12):3396–401.
- Hilgenbrink AR, Low PS. Folate receptor-mediated drug targeting: from therapeutics to diagnostics. *J Pharm Sci*. 2005;94(10):2135–46.
- Sudimack J, Lee RJ. Targeted drug delivery via the folate receptor. *Adv Drug Deliv Rev*. 2000;41(2):147–62.
- Mislick KA, Baldeschwieler JD, Kayyem JF, Meade TJ. Transfection of folate-polylysine DNA complexes: evidence for lysosomal delivery. *Bioconjug Chem*. 1995;6(5):512–5.
- Sohail MF, Hussain SZ, Saeed H, Javed I, Sarwar HS, Nadhman A, et al. Polymeric nanocapsules embedded with ultra-small silver nanoclusters for synergistic pharmacology and improved oral delivery of docetaxel. *Sci Rep*. 2018;8(1):13304.
- Shahnaz G, Perera G, Sakloetsakun D, Rahmat D, Bernkop-Schnürch A. Synthesis, characterization, mucoadhesion and biocompatibility of thiolated carboxymethyl dextran–cysteine conjugate. *J Control Release*. 2010;144(1):32–8.
- Saremi S, Atyabi F, Akhlaghi SP, Ostad SN, Dinarvand R. Thiolated chitosan nanoparticles for enhancing oral absorption of docetaxel: preparation, in vitro and ex vivo evaluation. *Int J Nanomedicine*. 2011;6:119.
- Kafedjiiski K, Krauland AH, Hoffer MH, Bernkop-Schnürch A. Synthesis and in vitro evaluation of a novel thiolated chitosan. *Biomaterials*. 2005;26(7):819–26.
- Iqbal J, Shahnaz G, Perera G, Hintzen F, Sarti F, Bernkop-Schnürch A. Thiolated chitosan: development and in vivo evaluation of an oral delivery system for leuprolide. *Eur J Pharm Biopharm*. 2012;80(1):95–102.
- Jiang L, Li X, Liu L, Zhang Q. Thiolated chitosan-modified PLA-PCL-TPGS nanoparticles for oral chemotherapy of lung cancer. *Nanoscale Res Lett*. 2013;8(1):1–11.
- Wang C, Huang Y. Facile preparation of fluorescent Ag-clusters–chitosan-hybrid nanocomposites for bio-applications. *New J Chem*. 2014;38(2):657–62.
- Ibrahim WM, AlOmrani AH, Yassin AEB. Novel sulphiride-loaded solid lipid nanoparticles with enhanced intestinal permeability. *Int J Nanomedicine*. 2014;9:129.
- Shahnaz G, Vetter A, Barthelmes J, Rahmat D, Laffleur F, Iqbal J, et al. Thiolated chitosan nanoparticles for the nasal administration of leuprolide: bioavailability and pharmacokinetic characterization. *Int J Pharm*. 2012;428(1–2):164–70.
- Laffleur F, Hintzen F, Rahmat D, Shahnaz G, Millotti G, Bernkop-Schnürch A. Enzymatic degradation of thiolated chitosan. *Drug Dev Ind Pharm*. 2013;39(10):1531–9.
- Carron P, Crowley A, O'Shea D, McCann M, Howe O, Hunt M, et al. Targeting the folate receptor: improving efficacy in inorganic medicinal chemistry. *Curr Med Chem*. 2018;25:2675–708.
- Fang G, Tang B, Chao Y, Xu H, Gou J, Zhang Y, et al. Cysteine-functionalized nanostructured lipid carriers for oral delivery of docetaxel: a permeability and pharmacokinetic study. *Mol Pharm*. 2015;12(7):2384–95.
- Gaikwad VL, Bhatia MS. Polymers influencing transportability profile of drug. *Saudi Pharm J*. 2013;21(4):327–35.
- Javed I, Hussain SZ, Ullah I, Khan I, Ateeq M, Shahnaz G, et al. Synthesis, characterization and evaluation of lecithin-based nanocarriers for the enhanced pharmacological and oral pharmacokinetic profile of amphotericin B. *J Mater Chem B*. 2015;3(42):8359–65.
- Saremi S, Dinarvand R, Kebriaeezadeh A, Ostad SN, Atyabi F. Enhanced oral delivery of docetaxel using thiolated chitosan nanoparticles: preparation, in vitro and in vivo studies. *Biomed Res Int*. 2013;2013:1–8.